The Journal of Chemical Physics

RESEARCH ARTICLE | OCTOBER 07 2016

The structural validity of various thermodynamical models of supercooled water

H. Pathak ; J. C. Palmer; D. Schlesinger ; K. T. Wikfeldt ; J. A. Sellberg ; L. G. M. Pettersson ; A. Nilsson

J. Chem. Phys. 145, 134507 (2016)
https://doi.org/10.1063/1.4963913

The structural validity of various thermodynamical models of supercooled water

H. Pathak,[1] J. C. Palmer,[2] D. Schlesinger,[1] K. T. Wikfeldt,[1] J. A. Sellberg,[3]
L. G. M. Pettersson,[1] and A. Nilsson[1]
[1]*Department of Physics, AlbaNova University Center, Stockholm University, SE-10691 Stockholm, Sweden*
[2]*Chemical and Biomolecular Engineering, University of Houston, Houston, Texas 77204-4004, USA*
[3]*Biomedical and X-Ray Physics, Department of Applied Physics, AlbaNova University Center, KTH Royal Institute of Technology, SE-10691 Stockholm, Sweden*

(Received 12 July 2016; accepted 19 September 2016; published online 7 October 2016)

The thermodynamic response functions of water exhibit an anomalous increase upon cooling that becomes strongly amplified in the deeply supercooled regime due to structural fluctuations between disordered and tetrahedral local structures. Here, we compare structural data from recent x-ray laser scattering measurements of water at 1 bar and temperatures down to 227 K with structural properties computed for several different water models using molecular dynamics simulations. Based on this comparison, we critically evaluate four different thermodynamic scenarios that have been invoked to explain the unusual behavior of water. The critical point-free model predicts small variations in the tetrahedrality with decreasing temperature, followed by a stepwise change at the liquid-liquid transition around 228 K at ambient pressure. This scenario is not consistent with the experimental data that instead show a smooth and accelerated variation in structure from 320 to 227 K. Both the singularity-free model and ice coarsening hypothesis give trends that indirectly indicate an increase in tetrahedral structure with temperature that is too weak to be consistent with experiment. A model that includes an apparent divergent point (ADP) at high positive pressure, however, predicts structural development consistent with our experimental measurements. The terminology ADP, instead of the commonly used liquid-liquid critical point, is more general in that it focuses on the growing fluctuations, whether or not they result in true criticality. Extrapolating this model beyond the experimental data, we estimate that an ADP in real water may lie around 1500 ± 250 bars and 190 ± 6 K. [http://dx.doi.org/10.1063/1.4963913]

I. INTRODUCTION

Water is one of the most important liquids and shows unusual behavior upon varying temperature and pressure.[1–3] This anomalous behavior is evident already at ambient conditions and becomes even more pronounced when water is cooled below the melting point of ice (0 °C or 273 K), where the liquid is metastable with respect to crystallization.[2,4,5] Of particular interest in this context is the temperature and pressure dependence of the thermodynamic response functions that are related to fluctuations in the liquid: the isothermal compressibility (κ_T), the specific heat capacity at constant pressure (C_p), and the thermal expansion coefficient (α_p).[2] The temperature dependence of κ_T and C_p has been decomposed into that of a normal liquid background and an anomalous contribution, where the latter shows an apparent power law divergence on approaching a seemingly singular temperature of about 228 K at ambient pressure.[6] In a similar manner, the enhancement of the correlation length κ_T obtained from small angle x-ray scattering has also been fitted to an apparent power law divergence of similar magnitude.[7]

Numerous scenarios have been proposed to explain the rapid increase in anomalous fluctuations in liquid water upon cooling. Here, we focus on four thermodynamically consistent scenarios that have proved challenging to scrutinize experimentally because of water's rapid crystallization kinetics in the deeply supercooled regime. Some of these hypotheses posit the existence of a metastable liquid-liquid transition (LLT) between a high-density and a low-density liquid state of water (HDL and LDL, respectively) that terminates in a liquid-liquid critical point (LLCP) at some specific temperature (T_C) and pressure (P_C).[1–3] According to the LLCP hypothesis, there is an LLCP at positive pressure and non-zero temperature.[8,9] Along the Widom line,[10] which is the extension of the LLT phase separation line beyond the LLCP, density fluctuations would reach a maximum in the one-phase region, consistent with equal population of molecules with HDL- and LDL-like local coordination environments.[11] Alternatively, in the critical point-free (CPF) model, the LLCP would instead occur at negative pressure.[1] The third scenario, the singularity-free (SF) model,[12] posits a continuous transformation without discontinuity, which would correspond to the LLCP being located at zero temperature and high positive pressure.[13] The fourth hypothesis, which has been the subject of recent debate,[14–18] posits that the enhanced fluctuations in supercooled water arise from the familiar liquid-solid transition[19–21] rather than from a metastable LLT and LLCP.

To evaluate these scenarios, various two-state thermodynamic models based on fluctuations in local HDL and LDL configurations in the liquid have been developed to describe water's properties in the supercooled regime, including its enhanced thermodynamic response functions.[22–24] From a phenomenological point of view, two-state models yield equations of state for supercooled water that can be fitted to agree remarkably well with experimental data.[22,25,26] Holten and Anisimov developed a two-state model with T_C and P_C as parameters to investigate how the location of an LLCP affects agreement with experimental thermodynamic data for water. Based on the fit to experiment,[22] they established bounds on the likely location of an LLCP in water, predicting that it lies in a broad P-T region centered at 130 bars and 227 K and extending between 217 K, 500 bars positive pressure and 235 K, −200 bars negative pressure.[22] The challenge for making extrapolations with such models is that they are fitted to data from experimental measurements performed far away from the apparent divergence temperature of 228 K. Recently, however, single-shot ultrafast x-ray scattering measurements using the Linac Coherent Light Source (LCLS) x-ray free-electron laser were performed on rapidly cooled, micron-sized droplets to probe liquid water's structure at temperatures down to 227 K at ambient pressure.[27] These experiments marked the first direct measurements of liquid water's structure in the previously inaccessible "no-man's land" region of its metastable phase diagram, which lies directly below the homogeneous ice nucleation line $T_H(P)$ ($T_H \approx 232$ K at ambient pressure[28]). Structural transformations in the liquid were monitored in this region by analyzing the height of the second peak in water's oxygen-oxygen pair-distribution function (O–O PDF), thereby elucidating changes in water's tetrahedrality as a function of temperature.

In the present study, we scrutinize hypothesized scenarios that have been invoked to explain water's thermodynamic anomalies by investigating the structural properties of several different water models using molecular dynamics (MD) simulations. The structural temperature dependence of the models is then compared with the now available experimental x-ray scattering data in "no-man's land" to gain insight into the plausibility of the various thermodynamic scenarios.

II. METHODS

A. Molecular dynamics simulations

Simulations of the TIP4P/2005 force-field were performed with 45 000 molecules using molecular dynamics in the isothermal–isobaric (NPT) ensemble. At low temperature, the simulations were run for up to 45 ns. A Nosé-Hoover thermostat and Parrinello–Rahman barostat were used to control the temperature and pressure, respectively, and a time step of 2 fs was applied (4 fs at the lowest temperatures). Long-range electrostatic interactions were treated with the particle-mesh Ewald method, long-range Lennard-Jones corrections were included, and the TIP4P/2005 intramolecular geometry was constrained using the LINCS algorithm. Gromacs 4.0 was used on a parallel platform for all simulations. Further details of the simulations can be found in Ref. 29 and its associated supplementary material. Simulations of the SPC/E model of water were performed using the GROMACS package ver. 4.5.3 for a temperature range of T = 200–370 K in steps of $\Delta T = 10$ K at 1 bar. Cubic simulation boxes of 512 molecules were equilibrated for $t_{equil} = 10$–100 ns in the NPT ensemble, depending on temperature. The simulations were run for a total of $t_{tot} = 1\mu s$ for temperatures equal to and below T = 230 K and for $t_{tot} = 500$ ns for higher temperatures using a time step of dt = 2 fs. The other settings were chosen as for the simulations of the TIP4P/2005 water model as described above. Further details can also be found in Ref. 27 and the associated supplementary material.

The iAMOEBA simulations were carried out using a cubic box of 500 molecules equilibrated at 298 K, 1 atm as the initial structure. iAMOEBA is a flexible model of water that uses point multipole electrostatics and an approximate description of electronic polarizability with up to three-body terms. A multiple time step velocity Verlet integrator was used to numerically integrate the equations of motion with a 0.5 fs and 2.0 fs time step for the bonded and nonbonded degrees of freedom, respectively. We use Langevin dynamics with a time constant of 1.0 ps^{-1} and a Monte Carlo barostat algorithm with a volume adjustment frequency of 25 steps in order to simulate the NPT ensemble. The MD simulations were run on NVIDIA C2070 graphics processing units with the OpenMM software. The simulation time for each point on the phase diagram ranged from 100 ns to 2.5 μs.

B. Hybrid Monte Carlo simulations

Hybrid Monte Carlo (HMC) simulations[30] were performed to compute the structural properties of monatomic water (mW)[21] and the variant of ST2 described by Poole *et al.*,[31] which uses the reaction field method[32] to treat long-ranged electrostatic interactions. Computational studies of mW report evidence of only a single liquid phase under deeply supercooled conditions.[33] By contrast, previous studies with this ST2 variant show that it exhibits metastable liquid-liquid phase separation below $T_c = 247 \pm 3$ K.[17,31] For consistency with these studies, we implemented mW and ST2 exactly as described in Refs. 33 and 31, respectively.

Sampling in the isothermal-isobaric ensemble was performed for systems with 512 water molecules by combining HMC moves consisting of short microcanonical molecular dynamics (MD) trajectories with standard log-volume displacement MC trials.[34] On average, a volume displacement was attempted once every four HMC moves. The HMC MD trajectories for mW were propagated using a velocity Verlet integrator[34] with a 16 fs time step, whereas the equations of motion for ST2 were integrated using the SETTLE algorithm[35] with a 4.25 fs time step. The length of the MD trajectories for mW and ST2 was set to 15 and 20 integration steps, respectively. This choice resulted in an average acceptance rate of ca. 30% for the HMC moves. The maximum size of the attempted volume perturbations was also set to achieve a similar acceptance rate for the log-volume displacement MC moves.

The mW and ST2 simulations were equilibrated for $\sim 10^5$ to 10^7 Monte Carlo Sweeps (MCS) depending on the state condition, where 1 MCS is defined as an attempted HMC or log-volume displacement move. The equilibration period was followed by a production phase of equal duration during which sampled configurations were saved for analysis. Following our previous studies of supercooled ST2, TIP5P, and TIP4P/2005 water,[16,36] structural relaxation times were analyzed at each state point to estimate the frequency at which statistically independent configurations were generated by the sampling protocol. We found that at least $\sim 10^3$ such configurations were generated at each state point during the production period, ensuring that sampling was sufficient to accurately estimate thermophysical properties from the resulting trajectories.

The LDL fraction was estimated using the molecular order parameter[23] $\zeta_i = r_0 - r_l$, where r_0 and r_l are the distances from the central molecule i to its first non-hydrogen-bonded neighbor (0) and to its last hydrogen-bonded neighbor (l), respectively. Neighboring molecules are defined to be hydrogen bonded if the distance between the oxygens on the donor (D) and acceptor (A) are within 0.35 nm and the H-D-A angle is less than 30°.[37] Russo and Tanaka[23] demonstrated that the ζ_i distribution is bimodal in the liquid region of TIP4P/2005 and TIP5P due to the presence of two populations of molecules with distinct local coordination environments. Following their analysis, we characterized these populations in ST2 by fitting the ζ_i distribution at each state point to two Gaussian populations using Eq. (3) in Ref. 23. The LDL fraction was then determined from the relative concentration of the Gaussian population centered at $\zeta_i > 0$ which consists of water molecules with a high degree of translational order in their second neighbor shell.

We note that different size simulation boxes have been used for the simulations with the TIP4P/2005 simulation using a two orders of magnitude bigger box with 45 000 molecules. The different box sizes used will, however, not affect the appearance of the second peak in the O–O PDF at 4.5 Å.

III. RESULTS AND DISCUSSION

We investigate the properties of different water models, including TIP4P/2005,[38] SPC/E,[39] iAMOEBA,[40] mW,[21] and ST2,[41] focusing on their tetrahedrality at supercooled temperatures and their consistency with the experimental isothermal compressibility data. The O–O PDF of water has a first peak at $r = 2.8$ Å and a second peak around $r = 4.5$ Å.[42–45] The location of the second peak in the O–O correlation is consistent with that of a second-nearest neighbor in tetrahedral symmetry and is therefore indicative of tetrahedrality.[27] In the following analysis, we use this second-nearest-neighbor peak as a measure of tetrahedral structure in water. In our previous study,[27] changes in tetrahedrality were monitored through the height, g_2, of the second peak. Here we eliminate differences in peak shape between the different models by defining an order parameter, A_2, obtained by integrating over a ca. 1 Å interval around the peak's maximum (supplementary material, Section SI.1).

Figure 1(a) shows A_2 values deduced from experimental data (supplementary material, Section SI.2) along with molecular simulation results for four different water models that will be described later in this section. The A_2 value for water's low-density amorphous (LDA) glass phase is also shown because it provides an upper bound to A_2, i.e., the maximum tetrahedrality that is expected to be observed in the liquid.

We observe that the water models can be divided into two groups based on comparison with the experiment. The iAMOEBA and TIP4P/2005 models predict variations in temperature dependence of A_2 that compare favorably with experiment; TIP4P/2005 exhibits a slightly smaller slope, whereas iAMOEBA almost overlaps the experimental data.

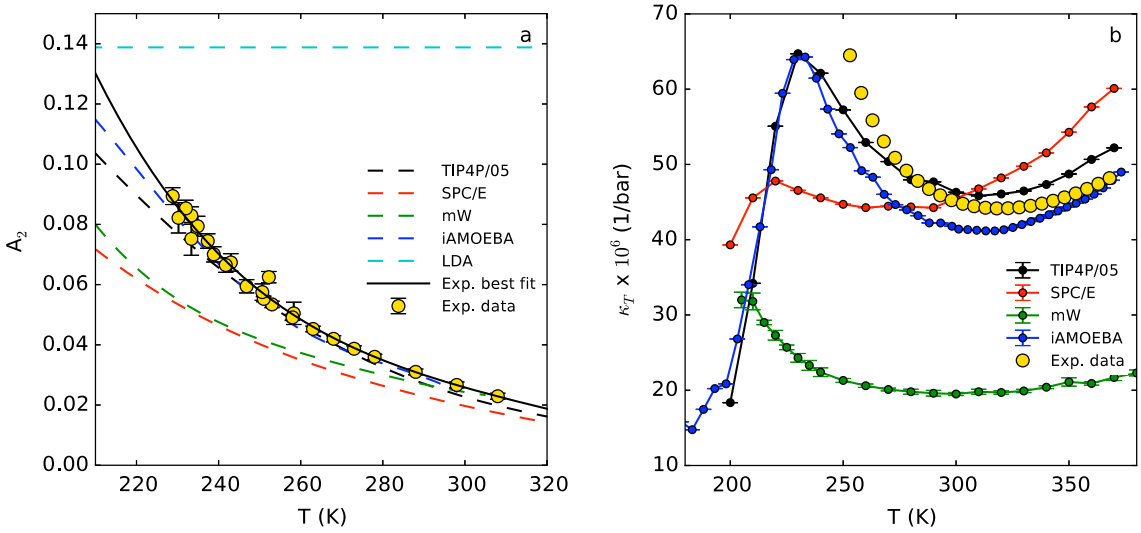

FIG. 1. (a) A_2 values for the TIP4P/2005, SPC/E, iAMOEBA, and mW water models compared to the experimental data. The A_2 value for LDA is also plotted as an indicator of the upper limit of A_2. (b) The isothermal compressibility of the different water models at ambient pressure. The TIP4P/2005 and iAMOEBA water models show a maximum in the isothermal compressibility at around 230 K. The SPC/E model shows a weak maximum at about 220 K while the mW model shows a continuous increase in the studied temperature range. The experimental data are taken from Ref. 46.

In contrast, SPC/E and mW show poor agreement with the experimental data, indicating that tetrahedrality develops too weakly in these models upon supercooling.

For comparison with variations in A_2, Fig. 1(b) shows experimental data for κ_T as a function of temperature[46] along with values of this quantity computed for the various water models. This comparison is only possible down to 249 K because no experimental data exist in the no-man's land region. We see that some models show a maximum at specific temperatures, that we denote $T_{\kappa T}^{max}$, i.e., 220 K for SPC/E, 230 K for TIP4P/2005, and 231 K for iAMOEBA. For the mW model, κ_T increases with decreasing temperature down to 200 K, beyond which the liquid becomes unstable with respect to crystallization and can no longer be equilibrated in the liquid state.[19,36] We again find that iAMOEBA and TIP4P/2005 capture the rapid increase in κ_T observed upon cooling real water, whereas temperature variations in κ_T predicted by the SPC/E and mW models are too weak. We note from the experimental data in Figs. 1(a) and 1(b) that an increase in tetrahedrality is accompanied by an increase in density fluctuations as indicated by κ_T.

The presence of an LLT has been demonstrated rigorously only for the ST2 model[16] and finite scaling would suggest an LLCP in the model; apparent divergence is observed in other models, but it is unknown if real criticality can develop on long enough length and time scales before the metastable liquid crystallizes.[47,48] A true critical point is characterized by diverging correlation length and specific values of critical exponents which become very challenging to determine both in simulations and even more so experimentally. We therefore adopt the terminology "apparent divergent point" (ADP) to denote when observations have suggested that thermodynamic response functions appear to diverge at a specific point in the P-T plane, which may or may not be characterized as an LLCP. Ultimately, only experiments will be able to provide definitive evidence on whether an observed ADP can be characterized as LLCP, i.e., whether fluctuations occur on large enough length and long enough time scales for criticality to develop. The Widom line is then simply defined as the locus of maxima in the thermodynamic response functions emanating from the ADP in the phase diagram. Here, we choose κ_T as the relevant response function and we define the temperature of maximum κ_T as $T_{\kappa T}^{max}$.

These models, i.e., mW, SPC/E, TIP4P/2005, and iAMOEBA, can now be placed into the context of the various scenarios to describe the anomalous properties of water. In order to do so, we first turn to the ST2 water model, which is overstructured compared to real water (i.e., exhibits anomalies at higher temperatures, see Fig. S3 of the supplementary material).[49,50] Equation of state calculations show, however, that ST2 qualitatively reproduces the anomalies of water and exhibits an ADP in the supercooled regime.[49,50] Recent free energy calculations unambiguously demonstrate that metastable liquid-liquid phase separation occurs in ST2 at temperatures below and at higher pressures than the ADP.[16–18,31,51,52] Finite size scaling behavior of ST2's LLT is also consistent with that expected for a first-order phase transition over the range of system sizes that can be explored with current computational resources.[14,16] Although these observations are consistent with the existence of an LLCP, the nature of the apparent critical singularity in ST2 has not been extensively scrutinized. It also remains to be seen if large-scale critical fluctuations can be equilibrated in ST2 before crystallization occurs. Nevertheless, the realization of an LLT and ADP in ST2 allows us to identify structural transformations in the liquid upon cooling that are consistent with the LLCP hypothesis.

Figure 2(a) shows the temperature dependence of A_2 at various pressures for the reaction field variant of the ST2 model described by Poole *et al.*[31] (ST2c according to the classification in Ref. 24). Figure 2(b) shows the LDL fraction as a function of temperature estimated using two-state population analysis described by Russo and Tanaka.[23] As temperature decreases at pressures above 2000 bars, ST2 initially exhibits only a modest increase in A_2 and the LDL fraction and then exhibits a jump as the LLT is reached. As

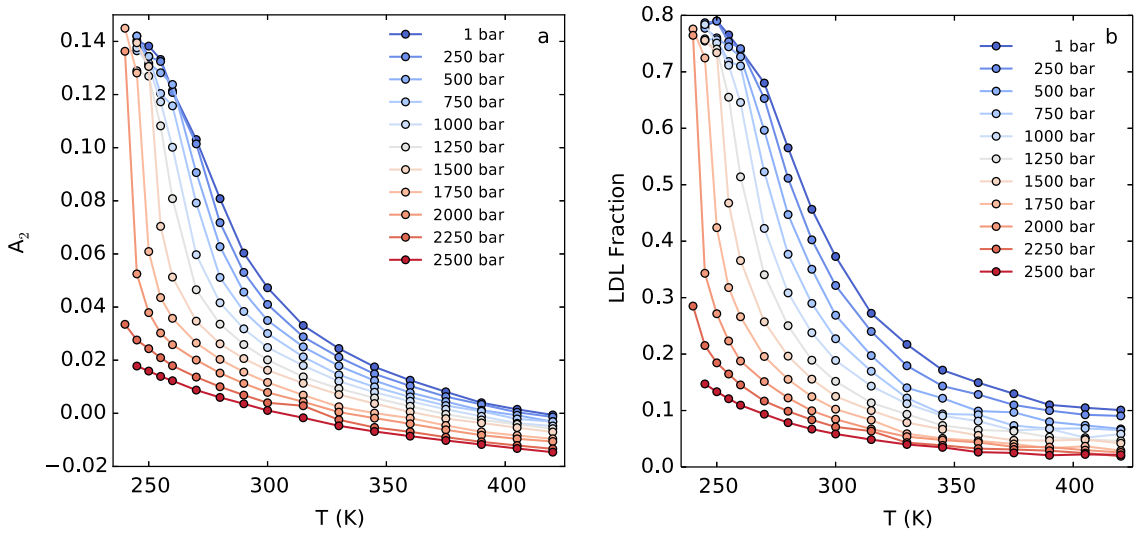

FIG. 2. (a) Isobars of A_2 vs temperature for the ST2 water model. (b) Isobars of LDL fraction vs temperature for the ST2 water model. The LDL fraction refers to the population of water molecules with LDL-like coordination environments.

pressure is reduced so the approach is beyond the ADP in the one-phase region, A_2 and the LDL fraction increase markedly upon cooling. A sharp increase is also observed in the slopes of both A_2 and the LDL fraction at around 1500 bars and 250-260 K, which is close to the reported ADP at 247 ± 3 K and pressure of 1850 ± 150 bars for ST2 water.[53] These results demonstrate the correspondence between the fraction of LDL-like molecules and tetrahedrality characterized by A_2, and they suggest that strong temperature variations in A_2 should be observed near an ADP and LLT.

The general trend in Fig. 2 is that for both A_2 and the LDL fraction, the slope diverges at the LLT and ADP and decreases as the temperature is increased in the one-phase region and, for both the LDL population and A_2, approach an overall linear variation with temperature far away from the ADP. This demonstrates that the fluctuations into tetrahedral LDL structures, as measured by the A_2 parameter or the LDL fraction, become very large only in a narrow range close to the ADP, while farther away in the one-phase region, the fluctuations become weaker as the pressure-temperature range affected by the ADP widens. This reflects the broadening of the anomalous region in the P-T plane and the weakening of the anomalous behavior as measurements or simulations are performed farther away from the ADP.[54]

The CPF model suggests that there is a spinodal associated with the first-order HDL-LDL transition at ambient pressure,[1] which is likely to be close to the estimated divergence temperature for C_p at ca. 228 K.[55] Based on the above results for ST2, one would expect a sharp change in A_2 around 228 K if the spinodal is encountered and much weaker temperature dependence of A_2 at higher temperatures. The experimental data show, however, a slower rise in A_2 around 228 K and higher tetrahedrality at temperatures above 228 K than predicted by the CPF model. The change in the O–O PDF upon undergoing an LLT is shown in Fig. S2c in the supplementary material.

The monatomic water (mW) force-field model describes water as a single particle and includes only short-range interactions.[21] For simulations of supercooled bulk mW using a simulation box of size larger than the critical nucleus for ice nucleation, there is no observation of an LLT at any pressure because the time scale for ice nucleation in the deeply metastable region is comparable to that associated with relaxation of the metastable liquid.[33,56] From Fig. 1(a), it is clear that the temperature dependence of the tetrahedrality of bulk liquid mW is much weaker than observed experimentally. Although the experimental data and κ_T values for mW appear to be offset in temperature and absolute magnitude, we find that mW predicts a much smaller rise in κ_T upon supercooling (Fig. 1(b)). We also note that A_2 curves for mW have the same shape at different pressures and only appear to shift slightly with respect to temperature (see supplementary material, Section SI.3). This behavior is in stark contrast to the abrupt changes in the shape of the A_2 curves that are observed as pressure is varied in the ST2 model. For mW, we find that there is no pressure where variations in tetrahedrality with temperature become even qualitatively similar to those observed in experiment. Furthermore, Fig. 1(b) shows that the rise in κ_T with decreasing temperature is also much smaller. These observations indicate that the temperature dependence of the fluctuations into tetrahedral structures in the mW model, i.e., the tetrahedrality as measured through A_2, is too weak to describe real water.

The singularity-free (SF) scenario for water proposes that the thermodynamic response functions do not diverge but remain finite at all temperatures.[12] In such a scenario, the negative derivative with temperature of the line of maximum density is sufficient to explain the anomalous behavior of thermodynamic functions. Based on the effects of hydrogen bond strength and cooperativity in a simple cell model of water, this scenario was related to an ADP at very high pressure and zero temperature.[13] Fig. 1(b) shows the temperature dependence of κ_T, where we see that the SPC/E model shows almost no rise in comparison to experiment; only a weak bump is observed around 220 K. This behavior suggests that the possible ADP for the SPC/E model is located very far from ambient conditions, which is consistent with previous studies that have estimated its location at 2.9 kbar and 130 K.[57] Because the ADP in SPC/E is located at very high pressure and low temperature, this model is closest to the SF scenario amongst the discussed models. As demonstrated in previous studies,[58] SPC/E underestimates the tetrahedral nature of real water, which is furthermore consistent with the modest change in A_2 with temperature (Fig. 1(a)) and the small increase of κ_T in this model. It is clear that the SPC/E model is inconsistent with the experimental data because it predicts an overly weak tendency towards fluctuations into tetrahedral structures as the temperature decreases into "no-man's land." Moving the ADP in the model to even lower temperature, or 0 K as in the SF scenario, would not be expected to increase the rate of structural transformation and fluctuations in the liquid, and in this sense the SPC/E model could be taken to indicate that the SF hypothesis is inconsistent with the experimental data. However, this is not a strict proof, but only an indication.

The iAMOEBA model is a variant of the polarizable AMOEBA water model[59] that treats the calculation of the induced dipoles in an approximate manner to reduce the computational cost associated with including polarizability. The model accurately predicts water's vapor, liquid, and solid state properties.[40] Similarly, the TIP4P/2005 model gives an excellent description of the phase diagram of water and ice and most thermodynamic properties. As shown in Fig. 1(b), TIP4P/2005 and iAMOEBA exhibit very similar behavior in κ_T, with a clear enhancement of fluctuations at the Widom line. Despite this similarity, iAMOEBA more accurately predicts experimental variations of A_2. From a computational perspective, iAMOEBA is also easier to equilibrate at temperatures below 230 K, where relaxations in TIP4P/2005 become extremely sluggish and frustrate accurate calculation of structural and thermophysical properties.[60] We therefore focus the remainder of our discussion on the iAMOEBA model. As shown in the supplementary material (Fig. S4), our analysis of κ_T and C_p for iAMOEBA suggests that it exhibits an ADP around 1750 ± 100 bars and 184 ± 3 K.

Figs. 3(a) and 3(b) show A_2 versus temperature at different pressures and isobaric derivatives of this function

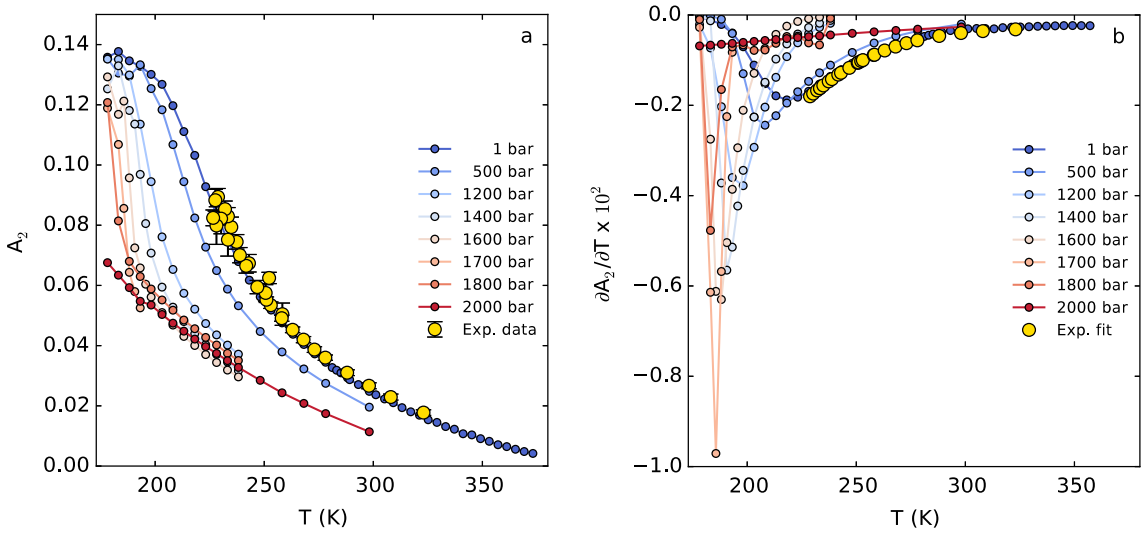

FIG. 3. (a) A_2 and (b) $\partial A_2/\partial T$ calculated from g_{O-O} (r) for the iAMOEBA water model.

$(\partial A_2/\partial T)_{P=constant}$, respectively. The behavior of A_2 for iAMOEBA is similar to that observed for ST2 water, consistent with both models exhibiting an ADP. The A_2 parameter increases with decreasing temperature, and the slope exhibits a minimum with respect to temperature (Fig. 3(b)). This minimum in the slope decreases and its location shifts to lower temperature upon increasing pressure. This trend continues until about 1700 bars, beyond which the minimum value of $\partial A_2/\partial T$ begins to increase with pressure. This non-monotonic behavior results in a global minimum in the slope around 1700 bars and 185-190 K (Fig. 3(b)), which is consistent with the existence of an ADP near these conditions. We also observe that the function $\partial A_2/\partial T$ computed for iAMOEBA at 1 bar agrees well with the experimental data, indicating that iAMOEBA accurately captures temperature-dependent variations in water's tetrahedrality. Based on predictions of the iAMOEBA model, we therefore posit that an ADP may exist in real water. The existence of such an ADP would, even if true criticality cannot develop, give rise to fluctuations extending into the ambient pressure regime, thereby explaining the strong temperature dependence of water's tetrahedrality. The question is the exact location of the ADP.

Having determined the location of the ADP in the iAMOEBA model, we need to relate the pressure scale of iAMOEBA to that of real water. To this end, we compare A_2 and $\partial A_2/\partial T$ for iAMOEBA at 1,500 and 1000 bars with the experimental data for real water at 1 bar (Figs. 4(a) and 4(b)). Here, we have shifted the temperature scales for the iAMOEBA data at 500 and 1000 bars such that the value of $T_{\kappa T}^{max}$ at both these pressures is aligned with the value of $T_{\kappa T}^{max}$ at 1 bar in order to compare the line shapes and slopes. After performing this temperature shift, we observe that the experimental data lie between the isobars at 1 bar and 500 bars for the iAMOEBA model. To check for consistency, we also inspect the κ_T temperature dependence using the same temperature shifts for data at 500 and 1000 bars (Fig. 4(c)). We find that the iAMOEBA data at 1 bar underestimate the sharpness of the rise of the experimental curve, whereas the iAMOEBA data at 500 and 1000 bars predict an overly sharp increase. This indicates that the iAMOEBA model seems to follow real water with a very modest shift in pressure of around 1-250 bars, suggesting that an ADP in real water may occur between 1500 and 1750 bars. This shift is consistent with the shift in the ice phase diagram for the iAMOEBA model.[40] Accounting for the temperature shift and estimated uncertainties, our analysis therefore suggests that an ADP could exist in real water at 1500 ± 250 bars and 190 ± 6 K.

We note that the computed values of A_2 and its derivative for the iAMOEBA model at 1,500, and 1000 bars begin to deviate from the experimental data at temperatures below 240 K, beyond which the magnitude of the deviation steadily increases as temperature decreases (Figs. 4(a) and 4(b)). This behavior illustrates the importance of obtaining experimental data below or close to the homogeneous ice nucleation temperature to evaluate water models, where the difference between such models becomes strong enough. Another essential point is that the experimental value of A_2 is higher than predicted by iAMOEBA at the model's $T_{\kappa T}^{max}$ of 231 ± 1 K at 1 bar. This discrepancy indicates that previous estimates of $T_{\kappa T}^{max}$ for real water, which are near the predicted diverging temperature of 228 K,[6] may need to be shifted to even higher temperatures. The previous estimates of $T_{\kappa T}^{max}$ are based on power law fits of available experimental data measured at temperatures far away from the apparent divergent temperature. Because the fit was likely only towards a maximum in a response function and not towards a point of true divergence, the exponent is unknown. Consequently, the uncertainty in the estimated apparent divergent temperature for real water is expected to be very large. We also note that $T_{\kappa T}^{max}$ may closely coincide with previous estimates of the homogeneous nucleation temperature of 232 K at 1 bar.[61] It is around $T_{\kappa T}^{max}$ that the change in tetrahedrality is the largest, suggesting that the population of LDL local structures is close to 50%. We anticipate that such an increase in the LDL concentration could explain the large increase in the ice nucleation rate observed at these conditions.[33]

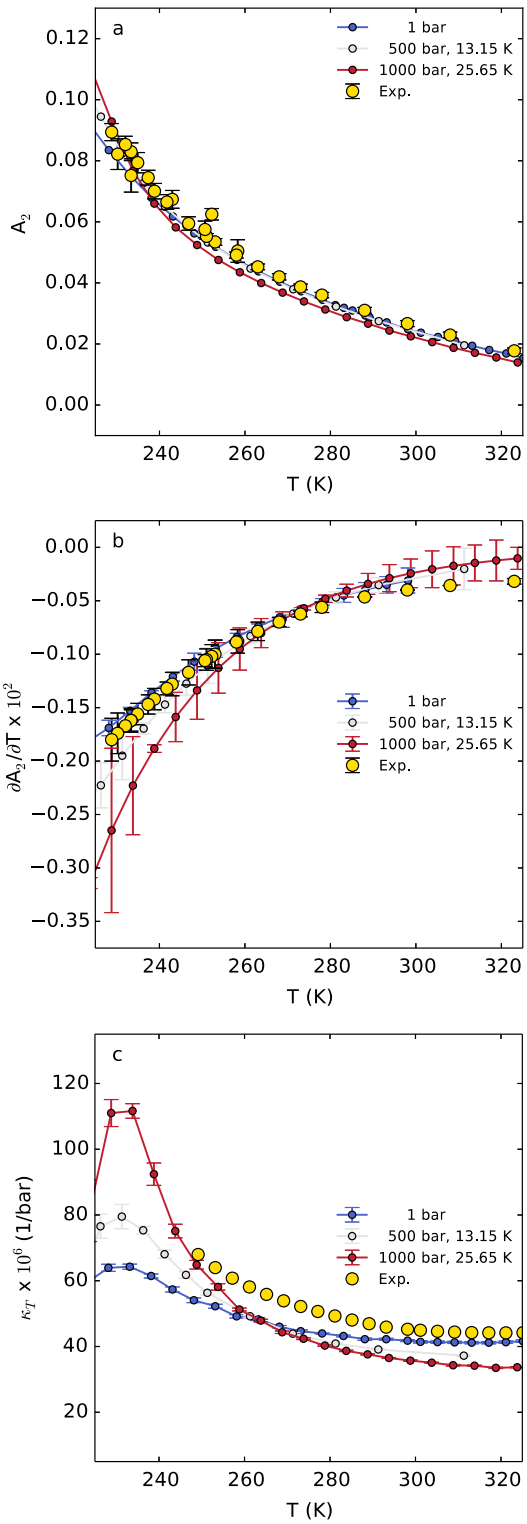

FIG. 4. (a) A_2 from experiment compared with isobars from the iAMOEBA water model. (b) $\partial A_2/\partial T$ from experiment compared with isobars from the iAMOEBA model. (c) Isothermal compressibility (κ_T) of water[46] compared with κ_T of the iAMOEBA water model. In all the figures, the temperature scales for 500 bars and 1000 bars have been shifted by 13.15 K and 25.65 K, respectively, so that $T_{\kappa T}^{max}$ for 500 bars and 1000 bars coincides with $T_{\kappa T}^{max}$ at 1 bar.

Holten and Anisimov[22] used a two-state description fitted to data for real water and concluded an ADP located at much lower pressure (ca. 130 bars) than the 1500 ± 250 bars predicted in the present study.[22] The variation of the LDL fraction with temperature at 1 bar was also estimated based on the two-state model[22] and gave a shape fully consistent with the proposed closeness to an ADP, i.e., similar to the iAMOEBA model at pressures close to its ADP in Fig. 3(a) with a low LDL fraction or A_2 value at temperatures far above $T_{\kappa T}^{max}$ followed by a rapid rise close to $T_{\kappa T}^{max}$. This is, however, inconsistent with the present experimental data for the A_2 variation with temperature at ambient pressure.

We also note a recent study by Ni and Skinner that used the E3B3 model[62] and obtained an ADP at 2.1 kbar and 180 K where the peak height g_2 at 1 bar as a function of temperature was evaluated and compared to the experimental data.[63] The agreement is good, but there is a small discrepancy in the supercooled region where the slope appears to be slightly less than for the experimental curve consistent with the ADP in the E3B3 model being further away towards higher pressure than what is estimated here for real water.

IV. CONCLUSIONS

Since the anomalous properties of water have been shown to be related to fluctuations into local tetrahedral structures,[2,3,22,23,27,54,64] we demonstrate here that structural properties can be used to test various thermodynamic models to explain the apparent divergence of the thermodynamic response functions at ambient pressure. In particular the temperature dependence of the 2nd shell in the O–O PDF has been experimentally derived[27] down to, and beyond, the previously estimated temperature where the response functions seem to diverge at 1 bar[6] allowing a basis for evaluating the various models. Here we introduce the concept of an apparent divergent point (ADP) meaning that there is a specific point in the water phase diagram where fluctuations between two competing local structures become enhanced in a way reminiscent of criticality and where these fluctuations extend over a large P-T neighborhood. The ADP could potentially be characterized as a liquid-liquid critical point (LLCP) if critical fluctuations could develop on sufficiently large length and sufficiently long time scales in this region where ice is the stable phase.[15,47] Based on different molecular dynamics models, we observe that the structural temperature dependence and, in particular, the area of the 2nd peak in the O–O PDF at 1 bar as a signature for the local tetrahedrality show a strong variation depending on where the ADP is located in the water phase diagram. If the ADP is at negative pressure with a liquid-liquid coexistence line extending to positive pressure, then the tetrahedrality should depend only weakly on temperature upon cooling until a sharp almost step-like increase is observed at the LLT. On the other hand, if the ADP moves to positive pressure, the transition beyond the ADP in the one-phase region becomes smoother with the temperature dependence becoming almost linear far enough away from the ADP.

Assuming an ADP at positive pressure, the tetrahedrality dependence becomes close to the experimental data at 1 bar. This scenario also gives reasonable agreement with experimental data for the isothermal compressibility, although

these measurements were conducted at higher temperatures. A model that lacks an ADP and where the fluctuations are instead related to fast ice nucleation on similar time scales as the equilibration in the liquid predicts too weak of a temperature dependence of both tetrahedrality and compressibility in comparison to experiment. Based on this comparison to experimental data, we conclude that the only scenario that gives a good consistency with the experimental data is when an ADP is included and located around 1500 ± 250 bars and 190 ± 6 K. However, the character of the ADP state point needs further investigation and eventually direct experimental measurements to reveal its true nature. Furthermore, the apparent divergent temperature of 228 K at 1 bar needs to be shifted to higher temperatures close to what has been previously denoted the homogeneous ice nucleation temperature around 232 K.

SUPPLEMENTARY MATERIAL

See the supplementary material for discussions about A_2 calculations for experimental data and for different water models.

ACKNOWLEDGMENTS

This work has been supported by the European Research Council (ERC) Advanced Grant under Project No. 667205, the Swedish National Research Council (VR) under Grant No. 2013-8823, and the Welch Foundation (Grant No. E-1882). Computational resources provided by the Swedish National Infrastructure for Computing (SNIC) are gratefully acknowledged. We thank Lee Ping Wang for providing the iAMOEBA water model data.

[1]C. A. Angell, Science **319**, 582 (2008).
[2]P. G. Debenedetti, J. Phys.: Condens. Matter **15**, R1669 (2003).
[3]O. Mishima and H. E. Stanley, Nature **396**, 329 (1998).
[4]C. A. Angell, Ann. Rev. Phys. Chem. **34**, 593 (1983).
[5]P. G. Debenedetti, *Metastable Liquids: Concepts and Principles* (Princeton University Press, 1996).
[6]R. J. Speedy and C. A. Angell, J. Chem. Phys. **65**, 851 (1976).
[7]C. Huang, T. M. Weiss, D. Nordlund, K. T. Wikfeldt, L. G. M. Pettersson, and A. Nilsson, J. Chem. Phys. **133**, 134504 (2010).
[8]O. Mishima and H. E. Stanley, Nature **392**, 164 (1998).
[9]P. H. Poole, F. Sciortino, U. Essmann, and H. E. Stanley, Nature **360**, 324 (1992).
[10]L. Xu, P. Kumar, S. V. Buldyrev, S.-H. Chen, P. H. Poole, F. Sciortino, and H. E. Stanley, Proc. Natl. Acad. Sci. U. S. A. **102**, 16558 (2005).
[11]K. T. Wikfeldt, A. Nilsson, and L. G. M. Pettersson, Phys. Chem. Chem. Phys. **13**, 19918 (2011).
[12]L. P. N. Rebelo, P. G. Debenedetti, and S. Sastry, J. Chem. Phys. **109**, 626 (1998).
[13]K. Stokely, M. G. Mazza, H. E. Stanley, and G. Franzese, Proc. Natl. Acad. Sci. U. S. A. **107**, 1301 (2010).
[14]T. A. Kesselring, G. Franzese, S. V. Buldyrev, H. J. Herrmann, and H. E. Stanley, Sci. Rep. **2**, 474 (2012).
[15]D. T. Limmer and D. Chandler, Mol. Phys. **113**, 2799 (2015).
[16]J. C. Palmer, F. Martelli, Y. Liu, R. Car, A. Z. Panagiotopoulos, and P. G. Debenedetti, Nature **510**, 385 (2014).
[17]F. Sciortino, I. Saika-Voivod, and P. H. Poole, Phys. Chem. Chem. Phys. **13**, 19759 (2011).
[18]F. Smallenburg and F. Scortino, Phys. Rev. Lett. **115**, 015701 (2015).
[19]D. T. Limmer and D. Chandler, J. Chem. Phys. **135**, 134503 (2011).
[20]D. T. Limmer and D. Chandler, J. Chem. Phys. **138**, 214504 (2013).
[21]V. Molinero and E. B. Moore, J. Phys. Chem. B **113**, 4008 (2009).
[22]V. Holten and M. A. Anisimov, Sci. Rep. **2**, 713 (2012).
[23]J. Russo and H. Tanaka, Nat. Commun. **5**, 3556 (2014).
[24]P. Gallo, K. Amann-Winkel, C. A. Angell, M. A. Anisimov, F. Caupin, C. Chakravarty, E. Lascaris, T. Loerting, A. Z. Panagiotopoulos, and J. Russo, Chem. Rev. **116**, 7463 (2016).
[25]H. Tanaka, J. Chem. Phys. **112**, 799 (2000).
[26]V. Holten, J. V. Sengers, and M. A. Anisimov, J. Phys. Chem. Ref. Data **43**, 043101 (2014).
[27]J. A. Sellberg, C. Huang, T. A. McQueen, N. D. Loh, H. Laksmono, D. Schlesinger, R. G. Sierra, D. Nordlund, C. Y. Hampton, D. Starodub, D. P. DePonte, M. Beye, C. Chen, A. V. Martin, A. Barty, K. T. Wikfeldt, T. M. Weiss, C. Caronna, J. Feldkamp, L. B. Skinner, M. M. Seibert, M. Messerschmidt, G. J. Williams, S. Boutet, L. G. M. Pettersson, M. J. Bogan, and A. Nilsson, Nature **510**, 381 (2014).
[28]H. Kanno and C. A. Angell, J. Chem. Phys. **70**, 4008 (1979).
[29]K. T. Wikfeldt, C. Huang, A. Nilsson, and L. G. M. Pettersson, J. Chem. Phys. **134**, 214506 (2011).
[30]S. Duane, A. D. Kennedy, B. J. Pendleton, and D. Roweth, Phys. Lett. B **195**, 216 (1987).
[31]P. H. Poole, R. K. Bowles, I. Saika-Voivod, and F. Sciortino, J. Chem. Phys. **138**, 034505 (2013).
[32]O. Steinhauser, Mol. Phys. **45**, 335 (1982).
[33]E. B. Moore and V. Molinero, Nature **479**, 506 (2011).
[34]D. Frenkel and B. Smit, *Understanding Molecular Simulation: From Algorithms to Applications*, 2nd ed. Computational Science Series Vol. 1 (Academic Press, San Diego, 2002).
[35]S. Miyamoto and P. A. Kollman, J. Comput. Chem. **13**, 952 (1992).
[36]J. C. Palmer, R. S. Singh, R. Chen, F. Martelli, and P. G. Debenedetti, "Density and bond-orientational relaxations in supercooled water," Mol. Phys. (published online 13 May 2016).
[37]A. Luzar and D. Chandler, Phys. Rev. Lett. **76**, 928 (1996).
[38]J. L. F. Abascal and C. Vega, J. Chem. Phys. **123**, 234505 (2005).
[39]H. J. C. Berendsen, J. R. Grigera, and T. P. Straatsma, J. Phys. Chem. **91**, 6269 (1987).
[40]L.-P. Wang, T. Head-Gordon, J. W. Ponder, P. Ren, J. D. Chodera, P. K. Eastman, T. J. Martinez, and V. S. Pande, J. Phys. Chem. B **117**, 9956 (2013).
[41]F. H. Stillinger and A. Rahman, J. Chem. Phys. **60**, 1545 (1974).
[42]A. H. Narten and H. A. Levy, J. Chem. Phys. **55**, 2263 (1971).
[43]L. B. Skinner, C. Huang, D. Schlesinger, L. G. M. Pettersson, A. Nilsson, and C. J. Benmore, J. Chem. Phys. **138**, 074506 (2013).
[44]A. V. Okhulkov, Y. N. Demianets, and Y. E. Gorbaty, J. Chem. Phys. **100**, 1578 (1994).
[45]L. B. Skinner, C. J. Benmore, J. C. Neuefeind, and J. B. Parise, J. Chem. Phys. **141**, 214507 (2014).
[46]G. S. Kell, J. Chem. Eng. Data **15**, 119 (1970).
[47]K. Binder, Proc. Natl. Acad. Sci. U. S. A. **111**, 9374 (2014).
[48]D. Chandler, Nature **531**, E1 (2016).
[49]V. Holten, J. C. Palmer, P. H. Poole, P. G. Debenedetti, and M. A. Anisimov, J. Chem. Phys. **140**, 104502 (2014).
[50]F. Smallenburg, P. H. Poole, and F. Sciortino, Mol. Phys. **113**, 2791 (2015).
[51]Y. Liu, J. C. Palmer, A. Z. Panagiotopoulos, and P. G. Debenedetti, J. Chem. Phys. **137**, 214505 (2012).
[52]Y. Liu, A. Z. Panagiotopoulos, and P. G. Debenedetti, J. Chem. Phys. **131**, 104508 (2009).
[53]M. J. Cuthbertson and P. H. Poole, Phys. Rev. Lett. **106**, 115706 (2011).
[54]A. Nilsson and L. G. M. Pettersson, Nat. Commun. **6**, 8998 (2015).
[55]C. A. Angell, W. J. Sichina, and M. Oguni, J. Phys. Chem. **86**, 998 (1982).
[56]E. B. Moore and V. Molinero, J. Chem. Phys. **130**, 244505 (2009).
[57]A. Scala, F. W. Starr, E. La Nave, F. Sciortino, and H. E. Stanley, Nature **406**, 166 (2000).
[58]S. Harrington, P. H. Poole, F. Sciortino, and H. E. Stanley, J. Chem. Phys. **107**, 7443 (1997).
[59]P. Ren and J. W. Ponder, J. Phys. Chem. B **107**, 5933 (2003).
[60]R. S. Singh, J. W. Biddle, P. G. Debenedetti, and M. A. Anisimov, J. Chem. Phys. **144**, 144504 (2016).
[61]B. J. Mason, Adv. Phys. **7**, 221 (1958).
[62]C. J. Tainter, L. Shi, and J. L. Skinner, J. Chem. Theory Comput. **11**, 2268 (2015).
[63]Y. Ni and J. L. Skinner, J. Chem. Phys. **144**, 214501 (2016).
[64]A. Nilsson, C. Huang, and L. G. M. Pettersson, J. Mol. Liq. **176**, 2 (2012).